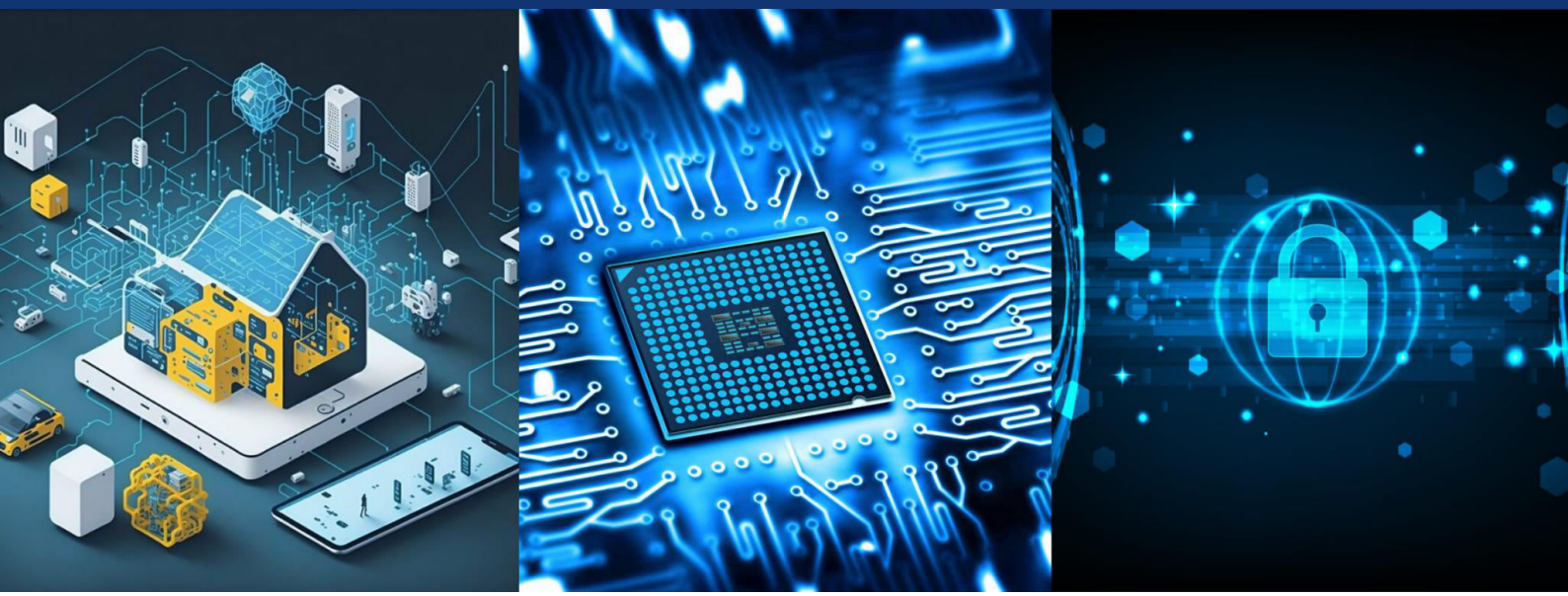
IJIRCCE

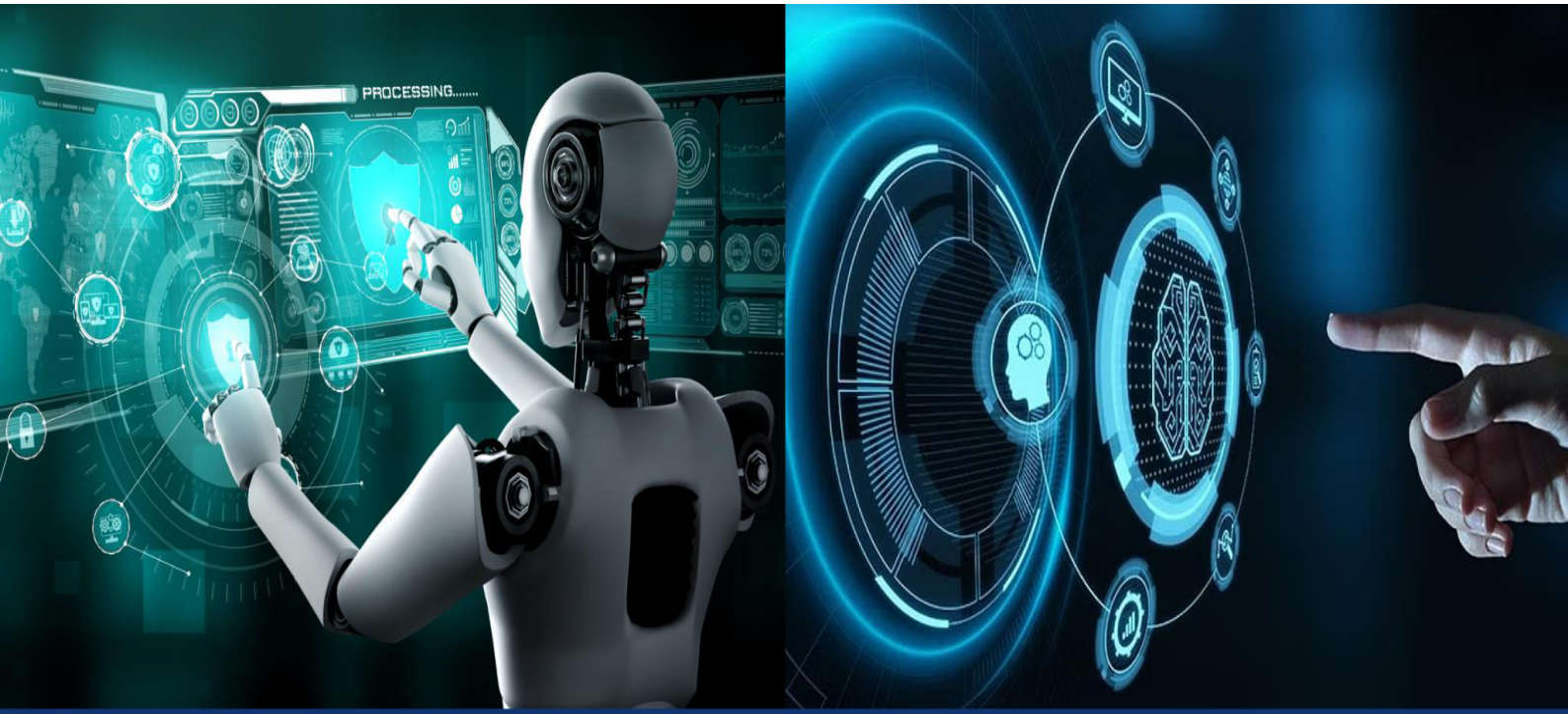
ISSN(O): 2320-9801

ISSN(P): 2320-9798



International Journal of Innovative Research in Computer and Communication Engineering

(A Monthly, Peer Reviewed, Refereed, Scholarly Indexed, Open Access Journal)



Impact Factor: 9.927

Volume 14, Issue 10, October 2026

© 2026 IJIRCCE | Volume 14, Issue 10, October 2026 DOI: 10.15680/IJIRCCE.2026.1410013

www.ijircce.com | e-ISSN: 2320-9801, p-ISSN: 2320-9798| Impact Factor: 9.927| ESTD Year: 2013|

International Journal of Innovative Research in Computer and Communication Engineering (IJIRCCE)

(A Monthly, Peer Reviewed, Refereed, Scholarly Indexed, Open Access Journal)

Face Recognition Using Visible, Thermal and Fused Images with LBP, PCA, SVM and Naive Bayes

Komal Gadekar[1], Sangeeta N. Kakarwal[2], Nitin S. Magar[3]

Master of Engineering, Department of Computer Science and Engineering, International Centre of Excellence in Engineering and Management, Chhatrapati Sambhajinagar, Maharashtra, India[1]

Professor, Department of Computer Science and Engineering, International Centre of Excellence in Engineering and Management, Chhatrapati Sambhajinagar, Maharashtra, India[2]

Assistant Professor, Department of Computer Science and Engineering, International Centre of Excellence in Engineering and Management, Chhatrapati Sambhajinagar, Maharashtra, India[3]

ABSTRACT: Visible face recognition can be affected by illumination and shadows, while thermal images capture emitted radiation and fused images provide complementary appearance information. This study evaluates a lightweight classical framework for unknown-ID face verification across Visible, Thermal and Fusion image conditions. Images are processed at 128 × 128 pixels with grayscale conversion and CLAHE. Local Binary Pattern (LBP) and Principal Component Analysis (PCA) representations are evaluated with linear Support Vector Machine (SVM) and Gaussian Naive Bayes, yielding twelve configurations. The updated experiment uses a subject-disjoint protocol: S01–S13 are used for training and S14–S17 are held out for testing, with zero subject overlap. Each reported modality is evaluated on 258 verification pairs. The strongest configuration is Visible LBP–SVM at 80.23% accuracy, followed by Visible PCA–SVM at 74.03% and Visible LBP–Naive Bayes at 70.93%. Thermal LBP–SVM reaches 68.60%, while Fusion LBP–SVM reaches 61.63%. These results describe the current saved unknown-ID test run and should not be compared as if they were the earlier image-level, subject-overlapping classification experiment.

I. INTRODUCTION

Face recognition is attractive for biometric identification because acquisition is contactless and can be implemented with conventional imaging hardware. Visible facial images contain fine texture and colour information but can change with illumination, shadows, pose, expression and partial occlusion. Thermal images encode emitted infrared radiation and are less dependent on ambient light, although they contain less visible-spectrum texture. The appearance gap between the sensing domains makes heterogeneous recognition a non-trivial classification problem [1]–[9].

Cross-spectral research has addressed this difficulty through mapping, synthesis, domain adaptation, deep metric learning and image fusion. Large public resources such as polarimetric thermal databases and ARL-VTF enable rigorous evaluation [3], [4]. However, many institutional projects operate with a small number of subjects, modest processors and limited paired data. In such settings, classical descriptors remain useful because their parameters are explicit, training cost is low and every stage can be reproduced without specialised hardware.

This work evaluates a controlled pipeline across three independent conditions while keeping preprocessing, image size and evaluation logic fixed. The conditions are Fusion Only, Thermal Only and Visible Only. LBP captures local texture transitions, whereas PCA models global directions of variance; each representation is paired with SVM and Gaussian Naive Bayes. Pre-generated fused images are treated as an input condition and their downstream effect on classification is measured.

The main contributions are a unified comparison of twelve feature–classifier configurations across three image conditions, a subject-disjoint unknown-ID evaluation protocol, and reproducible reporting of the saved test-run results.

© 2026 IJIRCCE | Volume 14, Issue 10, October 2026 DOI: 10.15680/IJIRCCE.2026.1410013

www.ijircce.com | e-ISSN: 2320-9801, p-ISSN: 2320-9798| Impact Factor: 9.927| ESTD Year: 2013|

International Journal of Innovative Research in Computer and Communication Engineering (IJIRCCE)

(A Monthly, Peer Reviewed, Refereed, Scholarly Indexed, Open Access Journal)

II. RELATED WORK

2.1 Thermal and Heterogeneous Face Recognition

Operational studies established that infrared imagery can support face recognition when visible-spectrum images deteriorate under poor illumination [7]–[9]. Subsequent work explored thermal-to-visible mappings, visible synthesis from thermal faces and cross-modal feature learning [5], [6], [27]–[29]. Hu et al. introduced a polarimetric thermal face database, and Poster et al. reported a large time-synchronised visible–thermal dataset that supports heterogeneous evaluation [3], [4]. These studies consistently identify alignment, data scarcity and modality discrepancy as major challenges.

2.2 Handcrafted Representations and Classical Classifiers

LBP encodes the sign of local intensity differences around a centre pixel and is widely used for texture analysis because of its low computational cost and relative robustness to monotonic intensity changes [10]. PCA projects high-dimensional image vectors onto orthogonal directions of maximum variance [11]. SVM is suitable for high-dimensional, small-sample classification because it maximises a separating margin [12]. Gaussian Naive Bayes provides a simple probabilistic baseline. CLAHE improves local contrast while limiting excessive amplification of histogram peaks [13].

2.3 Related Machine-Learning Context

Research by Kakarwal and collaborators provides additional context for supervised pattern recognition and analysis using multiple image sources. Retina and face recognition, database design, musical-instrument analysis and thermal face recognition have been studied using classical and neural approaches [16]–[20]. Related work also covers activity prediction, pancreas segmentation, early action prediction, brain-tumour analysis and spectroscopic soil classification [21]–[26].

2.4 Research Gap

Much of the recent heterogeneous-face literature emphasises large datasets and deep cross-modal embeddings. Comparatively fewer studies provide a tightly controlled small-data comparison in which local texture, global subspace features and two classifier assumptions are tested independently on visible, thermal and fused image sets using the same preprocessing and evaluation protocol. This gap motivates the present benchmark.

III. PROPOSED METHODOLOGY

3.1 Dataset Organisation and Experimental Design

The updated experiment uses identities S01–S17, divided by subject rather than by individual image. Subjects S01–S13 form the training group and S14–S17 form the unseen test group; the dashboard reports zero shared subjects. Visible, Thermal and Fusion conditions are evaluated independently with the same four feature–classifier combinations. The unknown-ID dashboard reports 258 verification test pairs per modality. The available image-list view shows 117 Thermal training images and 39 Thermal testing images; pair counts are verification-pair counts and must not be interpreted as image counts.

Table 1. Dataset composition and train–test allocation

Condition	Input type	Training subjects	Unseen test subjects / pairs
Visible	Visible-spectrum crops	S01–S13	S14–S17 / 258 pairs
Thermal	Thermal infrared crops	S01–S13	S14–S17 / 258 pairs
Fusion	Pre-generated fused crops	S01–S13	S14–S17 / 258 pairs

3.2 Image Pre-processing

Each image is converted to gray scale where required, resized to 128 × 128 pixels using area interpolation and enhanced using CLAHE with clipLimit = 2.0 and tileGridSize = (8, 8). The same preprocessing is used in every experimental branch.

$$I = 0.299R + 0.587G + 0.114B \quad (1)$$

$$z_j = (x_j - \mu_j) / \sigma_j \quad (2)$$

© 2026 IJIRCCE | Volume 14, Issue 10, October 2026 DOI: 10.15680/IJIRCCE.2026.1410013

www.ijircce.com | e-ISSN: 2320-9801, p-ISSN: 2320-9798| Impact Factor: 9.927| ESTD Year: 2013|

International Journal of Innovative Research in Computer and Communication Engineering (IJIRCCE)

(A Monthly, Peer Reviewed, Refereed, Scholarly Indexed, Open Access Journal)

The mean μ_j and standard deviation σ_j are learned from the training set and applied unchanged to the test set, preventing information leakage.

3.3 Local Binary Pattern Representation

Uniform LBP is computed using P = 48 sampling points at radius R = 6. Each 128 × 128 image is divided into 64 non-overlapping 16 × 16 blocks. Uniform LBP produces 50 histogram bins per block and therefore a 3,200-dimensional descriptor.

$$LBP_{p,r} = \sum_{p=0}^{P-1} s(g_p - g_c) \cdot 2^p; \quad s(t) = 1 \text{ if } t \geq 0, \text{ otherwise } 0 \tag{3}$$

$$\hat{h}_i = h_i / (\sum_j h_j + \varepsilon) \tag{4}$$

Face biometrics offer a practical way to verify identity without physical contact. Visible-spectrum cameras record facial detail, but the resulting appearance can vary with lighting, shadows, pose, expression and occlusion. Thermal sensors measure emitted infrared energy and can therefore retain useful facial patterns in lighting conditions that challenge ordinary cameras, although thermal images may contain less fine texture. Differences between visible and infrared imagery make cross-spectral face analysis difficult [1]–[9].

Researchers have investigated cross-spectral recognition through image translation, modality mapping, synthesis, domain adaptation, metric learning and fusion. Public datasets, including polarimetric thermal resources and ARL-VTF, support systematic evaluation [3], [4]. In smaller institutional studies, however, the number of subjects and paired samples may be limited. Classical feature descriptors are still useful in this setting because their operations are interpretable and can be run without specialised computing hardware.

$$C = (1 / (n - 1)) X_c^T X_c \tag{5}$$

$$C v_k = \lambda_k v_k \tag{6}$$

$$z = \Lambda_k^{-1/2} V_k^T (x - \mu) \tag{7}$$

This study compares three input conditions—Visible, Thermal and Fusion—under a common preprocessing and evaluation workflow. LBP represents local intensity patterns, while PCA describes variation in the overall image vector. Each representation is tested with linear SVM and Gaussian Naive Bayes. The fused images are treated as pre-existing inputs, so the experiment assesses their verification performance rather than proposing a new fusion algorithm.

A linear SVM with C = 10 is used for the reported configurations. The updated unknown-ID protocol evaluates verification pairs drawn from identities excluded from training.

$$\min \tfrac{1}{2} \|w\|^2 + C \sum_i \xi_i, \quad \text{subject to} \quad y_i(w^T x_i + b) \geq 1 - \xi_i, \quad \xi_i \geq 0 \tag{8}$$

3.6 Gaussian Naive Bayes Classifier

Gaussian Naive Bayes is included as a probabilistic baseline. All condition-specific scripts use var_smoothing = 10^{-5}.

$$\hat{c} = \arg\max_c P(c) \prod_j N(x_j; \mu_{cj}, \sigma^2_{cj}) \tag{9}$$

3.7 Evaluation Measures and Comparative Gain

$$\text{Accuracy} = (TP + TN) / (TP + TN + FP + FN) \tag{10}$$

$$\text{Precision} = TP / (TP + FP); \quad \text{Recall} = TP / (TP + FN); \quad F1 = 2PR / (P + R) \tag{11}$$

$$\text{Macro metric} = (1 / C) \sum_c \text{metric}_c \tag{12}$$

$$\Delta A = A_1 - A_0; \quad RI = ((A_1 - A_0) / A_0) \times 100\% \tag{13}$$

3.8 Experimental Setup

Table 2. Principal implementation settings

Component	Setting
Image size	128 × 128 pixels, gray scale
CLAHE	clipLimit = 2.0; tileGridSize = 8 × 8
LBP	uniform; P = 48; R = 6; block = 16 × 16; 3,200 features

© 2026 IJIRCCE | Volume 14, Issue 10, October 2026 DOI: 10.15680/IJIRCCE.2026.1410013

www.ijircce.com | e-ISSN: 2320-9801, p-ISSN: 2320-9798| Impact Factor: 9.927| ESTD Year: 2013|

International Journal of Innovative Research in Computer and Communication Engineering (IJIRCCE)

(A Monthly, Peer Reviewed, Refereed, Scholarly Indexed, Open Access Journal)

PCA	StandardScaler; whitening; maximum 150 components
Split	Subject-disjoint: train S01–S13; test S14–S17; zero shared subjects
SVM	linear kernel; C = 10 for all final scripts
Gaussian NB	var_smoothing = 10^{-5}
Software	Python, OpenCV, scikit-image/scikit-learn, NumPy, pandas, Matplotlib, joblib

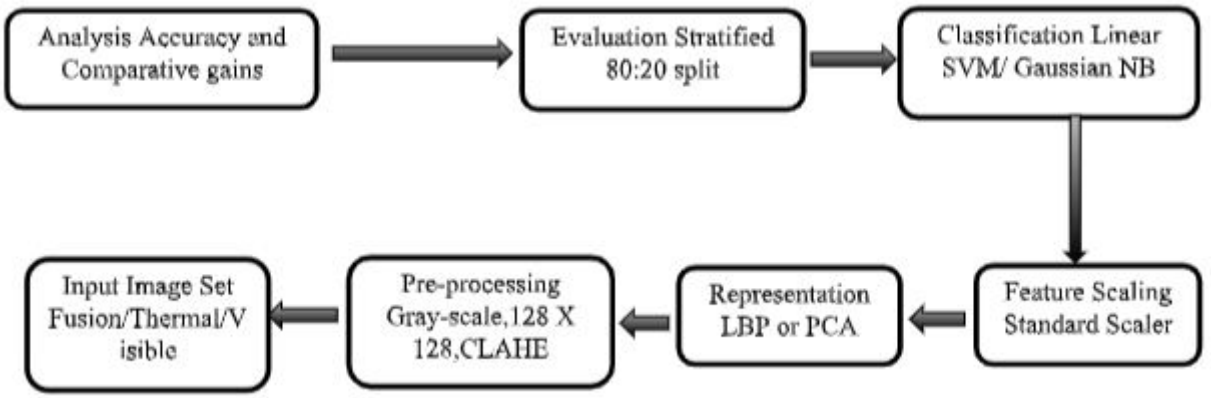


Figure 1. End-to-end process used for all three image conditions.

3.9 Training and Evaluation Procedure

Algorithm 1. Subject-disjoint unknown-ID verification benchmark

1. Assign subjects S01–S13 to training and S14–S17 to the unseen test group; verify that no subject occurs in both groups.
2. Prepare each modality independently using the documented grayscale conversion, 128 × 128 resizing and CLAHE preprocessing.
3. Generate the saved verification test pairs for each modality; the dashboard reports 258 test pairs per modality.
4. Compute LBP block histograms or fit PCA using training data only.
5. 2. RELATED WORK
6. Evaluate linear SVM or Gaussian Naive Bayes for each representation.
7. Thermal face analysis has been studied as an alternative when visible images are degraded by poor illumination [7]–[9]. Later work examined transformations between thermal and visible domains, synthesis of one modality from another, and cross-modal feature learning [5], [6], [27]–[29]. Publicly reported datasets include polarimetric thermal imagery and synchronised visible–thermal recordings [3], [4]. Across these studies, image alignment, limited paired data and differences between sensing domains remain important evaluation challenges.
8. Save the result outputs and use the same frozen test pairs for comparisons.
9. LBP summarises local texture by encoding whether neighbouring pixels are brighter or darker than a centre pixel; this makes it computationally economical for texture description [10]. PCA instead finds orthogonal directions that explain variation in the training data [11]. SVM learns a decision boundary by maximising its margin, while Gaussian Naive Bayes provides a probabilistic baseline based on conditional feature independence. CLAHE is used to improve local contrast without allowing histogram peaks to grow without control [12], [13].

© 2026 IJIRCCE | Volume 14, Issue 10, October 2026 DOI: 10.15680/IJIRCCE.2026.1410013

www.ijircce.com | e-ISSN: 2320-9801, p-ISSN: 2320-9798| Impact Factor: 9.927| ESTD Year: 2013|

International Journal of Innovative Research in Computer and Communication Engineering (IJIRCCE)

(A Monthly, Peer Reviewed, Refereed, Scholarly Indexed, Open Access Journal)

IV. RESULTS

4.1 Overall Classification Accuracy

Table 3 reports the twelve configurations from the saved subject-disjoint unknown-ID dashboard. Visible LBP–SVM achieves the highest accuracy (80.23%). Thermal LBP–SVM reaches 68.60%, and Fusion LBP–SVM reaches 61.63%. Every modality uses the same reported count of 258 test pairs.

Table 3. Updated subject-disjoint unknown-ID verification results

Modality	Feature	Classifier	Accuracy
Visible	LBP	SVM	80.23%
Visible	LBP	Naive Bayes	70.93%
Visible	PCA	SVM	74.03%
Visible	PCA	Naive Bayes	65.50%
Thermal	LBP	SVM	68.60%
Thermal	LBP	Naive Bayes	57.75%
Thermal	PCA	SVM	51.94%
Thermal	PCA	Naive Bayes	51.16%
Fusion	LBP	SVM	61.63%
Fusion	LBP	Naive Bayes	51.94%
Fusion	PCA	SVM	54.65%
Fusion	PCA	Naive Bayes	52.33%

Handcrafted features and conventional classifiers

4.2 Condition Gain Analysis

Using LBP–SVM, Visible reaches 80.23%, Thermal reaches 68.60%, and Fusion reaches 61.63%. Visible is 11.63 percentage points above Thermal and 18.60 points above Fusion. Thermal is 6.97 points above Fusion. These are absolute differences between the three independently evaluated modality-specific models, not evidence that image fusion itself causes a performance reduction.

Comparison	Absolute gain (pp)	Relative improvement (%)
Visible vs Thermal (LBP–SVM)	11.63	16.95
Visible vs Fusion (LBP–SVM)	18.60	30.18
Thermal vs Fusion (LBP–SVM)	6.97	11.31

4.3 Effect of Representation and Classifier

Visible LBP–SVM is the strongest of the twelve configurations at 80.23%. Within Visible, PCA–SVM reaches 74.03%, LBP–Naive Bayes 70.93%, and PCA–Naive Bayes 65.50%. For Thermal, LBP–SVM leads at 68.60%; the remaining configurations range from 51.16% to 57.75%. For Fusion, LBP–SVM reaches 61.63%, while the other three configurations range from 51.94% to 54.65%. The ranking indicates that the best feature–classifier combination depends on the input condition.

V. DISCUSSION

The saved unknown-ID results show a clear difference between modalities. Visible LBP–SVM provides the best result (80.23%), while Thermal LBP–SVM reaches 68.60% and Fusion LBP–SVM reaches 61.63%. Since test identities S14–S17 are excluded from training, the evaluation is more demanding than a random image-level split that allows the same identities in both sets. The figures should be interpreted as verification performance on the current subject-disjoint pair set, not as general population-level biometric performance.

Fusion images were generated before classification; therefore, this study measures the downstream verification performance of the available fused images and does not propose a new fusion operator. The classical pipeline remains

www.ijircce.com | e-ISSN: 2320-9801, p-ISSN: 2320-9798| Impact Factor: 9.927| ESTD Year: 2013|

International Journal of Innovative Research in Computer and Communication Engineering (IJIRCCE)

(A Monthly, Peer Reviewed, Refereed, Scholarly Indexed, Open Access Journal)

relatively lightweight, but the current results also show that fused inputs do not automatically outperform visible or thermal inputs. Differences may reflect image quality, alignment, sample composition and the fusion process.

VI. CONCLUSION AND LIMITATIONS

This paper reports a classical unknown-ID face-verification benchmark using LBP and PCA with linear SVM and Gaussian Naive Bayes on Visible, Thermal and Fusion images. With a subject-disjoint split (training subjects S01–S13; unseen test subjects S14–S17; zero shared subjects), the strongest saved result is Visible LBP–SVM at 80.23%, followed by Visible PCA–SVM at 74.03%. Thermal LBP–SVM achieves 68.60%, and Fusion LBP–SVM achieves 61.63%. The reported dashboard evaluates 258 verification pairs per modality.

Important limitations remain. Only four identities are held out for testing, and the result depends on the composition of the saved verification pairs and the decision threshold used by the dashboard. The reported scores should not be interpreted as population-level biometric performance. The dataset and pair-generation procedure should be documented fully, near-duplicate and cross-condition correspondences should be audited, and results should ideally be repeated across additional subject-disjoint splits. Precision, recall and F1 values should be reported exactly as produced by the same frozen run; they should not be mixed with metrics from the earlier experiment.

Despite these limitations, the updated experiment provides a transparent comparison of twelve classical feature–classifier configurations under an explicit unseen-identity test protocol. The saved results establish Visible LBP–SVM as the strongest configuration in this run, while also showing that thermal and fused inputs remain challenging under the subject-disjoint setting.

The research gap addressed here is a controlled comparison of local-texture and global-subspace representations with two conventional classifiers across visible, thermal and pre-generated fused face images. The same input preparation and a subject-disjoint unknown-ID test protocol are used to make the twelve configurations directly comparable within this dataset.

REFERENCES

[1] D. Anghelone, C. Chen, A. Ross, and A. Dantcheva, “Beyond the visible: A survey on cross-spectral face recognition,” arXiv:2201.04435, 2022.
[2] X. Wang, J. Peng, S. Zhang, B. Chen, Y. Wang, and Y. Guo, “A survey of face recognition,” arXiv:2212.13038, 2022.
[3] S. Hu et al., “A polarimetric thermal database for face recognition research,” in Proc. IEEE Conf. Computer Vision and Pattern Recognition Workshops (CVPRW), 2016, pp. 119–126.
[4] D. Poster et al., “A large-scale, time-synchronized visible and thermal face dataset,” in Proc. IEEE/CVF Winter Conf. Applications of Computer Vision (WACV), 2021, pp. 1559–1568.
[5] M. S. Sarfraz and R. Stiefelhagen, “Deep perceptual mapping for thermal to visible face recognition,” arXiv:1507.02879, 2015.
3. PROPOSED METHODOLOGY
[7] D. A. Socolinsky and A. Selinger, “Thermal face recognition in an operational scenario,” in Proc. IEEE Conf. Computer Vision and Pattern Recognition, 2004, pp. 1012–1019.
[8] R. S. Ghiass, O. Arandjelović, A. Bendada, and X. Maldague, “Infrared face recognition: A comprehensive review of methodologies and databases,” Pattern Recognition, vol. 47, no. 9, pp. 2807–2824, 2014.
[9] X. Chen, P. J. Flynn, and K. W. Bowyer, “Infrared and visible face recognition,” Computer Vision and Image Understanding, vol. 99, no. 3, pp. 332–358, 2005.
[10] T. Ojala, M. Pietikäinen, and T. Mäenpää, “Multiresolution gray-scale and rotation invariant texture classification with local binary patterns,” IEEE Trans. Pattern Analysis and Machine Intelligence, vol. 24, no. 7, pp. 971–987, 2002.
[11] M. Turk and A. Pentland, “Eigenfaces for recognition,” Journal of Cognitive Neuroscience, vol. 3, no. 1, pp. 71–86, 1991.
[12] C. Cortes and V. Vapnik, “Support-vector networks,” Machine Learning, vol. 20, pp. 273–297, 1995.
[13] K. Zuiderveld, “Contrast limited adaptive histogram equalization,” in Graphics Gems IV, P. S. Heckbert, Ed. Academic Press, 1994, pp. 474–485.

www.ijircce.com | e-ISSN: 2320-9801, p-ISSN: 2320-9798| Impact Factor: 9.927| ESTD Year: 2013|

International Journal of Innovative Research in Computer and Communication Engineering (IJIRCCE)

(A Monthly, Peer Reviewed, Refereed, Scholarly Indexed, Open Access Journal)

[14] X. Zhang et al., "VIFB: A visible and infrared image fusion benchmark," in Proc. IEEE/CVF Conf. Computer Vision and Pattern Recognition Workshops, 2020.
[15] A. George and S. Marcel, "Lightweight cross-spectral face recognition via contrastive alignment and distillation," arXiv:2605.04769, 2026.
[16] S. N. Kakarwal and R. R. Deshmukh, "Analysis of retina recognition by correlation and covariance matrix," in Proc. Third International Conference on Emerging Trends in Engineering and Technology, Goa, India, 2010, pp. 496–499.
[17] S. N. Kakarwal and R. R. Deshmukh, "Face recognition using supervised learning," in Proc. WorldComp 2012, Las Vegas, USA, July 2012.
[18] M. M. Ambekar, S. N. Kakarwal, and S. S. Khedgikar, "Design, acquisition and collection of multiple-source databases to increase accuracy and level of security," in Proc. IEEE International Conference ICSIDEMPC, 2020.
[19] S. R. Choudhari and S. N. Kakarwal, "Analysis of musical string instruments using k-NN," in Proc. IEEE International Conference ICSIDEMPC, 2020.
[20] S. N. Kakarwal, K. P. Choudhari, and R. B. Patil, "Face recognition based on supervised learning," in Proc. IEEE International Conference ICSIDEMPC, 2020.
[21] S. N. Kakarwal and A. S. Gawali, "Context aware human activity prediction in videos using hand-centric features and dynamic programming-based prediction algorithm," Journal of Integrated Science and Technology, vol. 10, no. 1, pp. 11–17, 2022.
[22] S. N. Kakarwal and P. M. Paithane, "Automatic pancreas segmentation using ResNet-18 deep learning approach," System Research and Information Technologies, no. 2, pp. 104–116, 2022, doi: 10.20535/SRIT.2308-8893.2022.2.08.
[23] A. Gawali and S. N. Kakarwal, "Enhancing early action prediction in videos through temporal composition of sub-actions," Multimedia Tools and Applications, vol. 84, no. 8, pp. 4253–4281, published online 18 Mar. 2024, doi: 10.1007/s11042-024-18870-0.
[24] S. N. Kakarwal, R. Mapari, A. K. Jain, V. Sharma, P. P. Mane, J. R. Raja Kumar, and R. K. Pradhan, "Enhanced detection and segmentation of brain tumors using a Dense BW-CNN approach," Journal of Engineering, vol. 2024, Article 1622294, 14 pages, 2024, doi: 10.1155/2024/1622294.
Each input image is converted to grayscale when needed, resized to 128 × 128 pixels using area interpolation, and enhanced with CLAHE (clipLimit 2.0; tileGridSize 8 × 8). Keeping these operations consistent across modalities reduces differences caused by preprocessing choices.
[26] S. N. Kakarwal, C. M. Gaikwad, and A. N. Ghule, "Classification based on soil attributes using non-imagery spectroscopic data," in Proc. ICKE 2023, Dr. Babasaheb Ambedkar Marathwada University, Chhatrapati Sambhajinagar, India, 8–9 May 2023.
[27] F. Juefei-Xu et al., "NIR-VIS heterogeneous face recognition via cross-spectral joint dictionary learning and reconstruction," in Proc. IEEE Conf. Computer Vision and Pattern Recognition Workshops, 2015.
[28] C. Reale, N. M. Nasrabadi, H. Kwon, and R. Chellappa, "Deep heterogeneous face recognition networks based on cross-modal distillation and an equitable distance metric," in Proc. IEEE Conf. Computer Vision and Pattern Recognition Workshops, 2017.
[29] T. de Freitas Pereira and S. Marcel, "Heterogeneous face recognition using inter-session variability modelling," in Proc. IEEE Conf. Computer Vision and Pattern Recognition Workshops, 2016.
[30] K. Chaudhari, "Development of Thermal Infrared and Visible Imagery Face Database," Copyright Office, Government of India, Copyright Diary No. 23164/2024-CO/L, Registration No. L-154687/2024, registered 27 September 2024.



INTERNATIONAL STANDARD SERIAL NUMBER INDIA

INNO SPACE SJIF Scientific Journal Impact Factor

doi crossref

निस्केयर NISCAIR

INTERNATIONAL JOURNAL OF INNOVATIVE RESEARCH

IN COMPUTER & COMMUNICATION ENGINEERING

9940 572 462 6381 907 438 ijircce@gmail.com

www.ijircce.com

Scan to save the contact details